FLOW TECHNIQUES, MEDICAL

Ultrasound is routinely used as a clinical tool for diagnosing and assessing blood-flow-related problems. Common applications include echocardiac imaging of flows within the heart, obstetric measurement of blood flow to the fetus in the umbilical cord, diagnosis of peripheral vascular diseases in arteries and veins, and assessment of cerebral circulation. The primary reason for the popularity of ultrasonic flow measurement in its noninvasive nature. Flow is measured by placing a transducer on the surface of the body and directing the ultrasound beam at the vessel of interest. From both the physician's and the patient's points of view, the measurements are quick, simple, and safe, with a minimum of discomfort to the patient. Other blood flow measurement methods, such as dye-dilution or the electromagnetic flowmeter, require injection and sampling of dye into the bloodstream or surgically placing a probe around the blood vessel in question.

There are a number of different types of ultrasonic flow measurement systems. The simplest is a continuous-wave device with an audio output; this system costs a few thousand

J. Webster (ed.), *Wiley Encyclopedia of Electrical and Electronics Engineering*. Copyright © 1999 John Wiley & Sons, Inc.

dollars. The most complex is a color flow mapping system, capable of integrating a color image of flow with a gray-scale image of anatomy; this system costs a few hundred thousand dollars. Most systems are designed for transcutaneous measurements, but specialized ultrasound probes for transesophageal, transrectal, transvaginal, and intravascular flow measurement are also available.

Current commercial systems operate with ultrasound frequencies in the 1 to 10 MHz frequency range. This frequency range has been determined by tissue parameters such as the ultrasound attenuation, which increases with frequency. At frequencies above 10 MHz, the attenuation is high, which limits the depth penetration of ultrasound into the body. The ultrasound frequency, along with the speed of sound in tissue and the transducer element size, determines the spatial resolution of the flow measurements. At frequencies below 1 MHz, the resolution is too poor to be useful.

Currently, there are two primary ultrasonic flow measurement techniques: Doppler and time-domain correlation. The first systems, as well as the large majority of current systems, are all Doppler based. These systems all transmit ultrasound of a given frequency into the body and calculate the flow velocity from the frequency of the reflected ultrasound echoes. Time domain correlation techniques are more recent and calculate the flow velocity from the change in transit time, rather than the change in frequency, of reflected echoes.

DOPPLER BLOOD FLOW MEASUREMENT

Doppler Effect

The Doppler effect was first described by Hans Christian Doppler (1803–1853) in a paper presented to the Royal Society of Learning in 1842 and published the following year (1). Doppler postulated that the colored appearance of stars was a result of the relative motion of the stars with respect to earth. This relative motion will cause a change in frequency of the light received from the star, causing it to appear bluish for motion toward the earth and reddish for motion away from the earth. Doppler's theory was validated by Buys Ballot in 1845, and the Doppler effect is used extensively in astronomy, meteorology, and radar, as well as medical applications of flow measurement (ironically, Doppler was wrong about the colored appearance of stars, which is a result of temperature rather than relative motion to the earth).

The first ultrasonic Doppler blood flow measurement was developed by Satomura (2) in 1957. He found that ultrasound reflected from moving blood cells differs in frequency from that transmitted and that the frequency difference is related to the blood flow rate. Satomura's system, as well as all ultrasound flow measurement systems, uses an acoustic transducer to propagate an ultrasound beam into the body. A Doppler shift in the frequency of the transmitted ultrasound will occur for tissues within the beam that are moving toward or away from the front of the transducer. Usually the tissue of interest is flowing blood, where the primary source of scatterers are red blood cells; but other structures, such as moving vessel walls, also contribute to the Doppler shift. When the acoustic transducer transmits ultrasound with frequency f_t, reflected echoes from blood cells moving toward the transducer will have a higher frequency than f_t, and those moving away from the transducer will have a lower frequency. In practice, blood cells move through the beam at an angle θ with respect to the beam axis. In this case, only the flow component in the direction of the ultrasound beam contributes to the Doppler shift. If the angle θ is known, the resulting reflected signal frequency f_r is

$$f_r = f_t + f_D = f_t \frac{c + V\cos\theta}{c - V\cos\theta} \tag{1}$$

where c is the speed of sound in blood, V is the velocity of the scatterer, and f_D is the Doppler shift. The speed of sound in soft tissue and blood (approximately 1540 m/s) is much greater than blood flow velocities in the body, and the Doppler frequency is simplified to

$$f_D = \frac{2f_t V\cos\theta}{c} \tag{2}$$

and the scatterer velocity, to

$$V = \frac{f_D c}{2f_t\cos\theta} \tag{3}$$

Note that Doppler flow measurements cannot be made at $\theta = 90°$ because the cosine term becomes zero. This is a limitation of single-beam ultrasound flow measurements, the transducer flow angles near 90° are avoided if possible.

Doppler Spectrum

Velocity Spread. In practice, the Doppler-shifted signal received from flowing blood is never a single frequency but rather a band of frequencies, referred to as the Doppler spectrum. The Doppler spectrum originates for a number of reasons (3). First, there is not just one but many erythrocytes within the ultrasound beam, each moving with a potentially different velocity. Under ideal conditions, the power of a particular frequency in the Doppler spectrum is proportional to the number of erythrocytes moving with the velocity producing that particular Doppler shift. Velocity profiles within a blood vessel are rarely uniform, ranging from somewhat parabolic in veins to turbulent in large arteries. This means that there will be a velocity spread present in the ultrasound beam, with a corresponding spread of Doppler shift frequencies. Figure 1 shows the Doppler spectrum measured in the femoral artery at six different locations in the cardiac cycle. At 0°, the flow profile is nearly flat, indicating that most of the blood cells are traveling at the same velocity. The corresponding Doppler spectrum has a sharp and high-amplitude peak at F_{V1}, which is the frequency corresponding to V_1. At 60°, the flow has reversed with a wider range of flow velocities, and the corresponding Doppler spectrum has negative frequencies and is much broader. The magnitude of F_{V2} at 60° is smaller than F_{V1} at 0°, because a smaller number of scatterers are traveling at that velocity. The Doppler spectrum changes its shape accordingly for the other flow profiles (120° through 300°) present throughout the cardiac cycle.

Frequency-Dependent Properties of Tissue. The shape of the Doppler spectrum is also affected by factors not directly related to blood flow velocity, such as ultrasonic tissue properties. The attenuation of ultrasound in tissue increases with frequency, with attenuation in soft tissue (≈0.8 dB/cm-MHz) much greater than that in blood (≈0.2 dB/cm-MHz). Thus the higher-frequency components will be attenuated more from

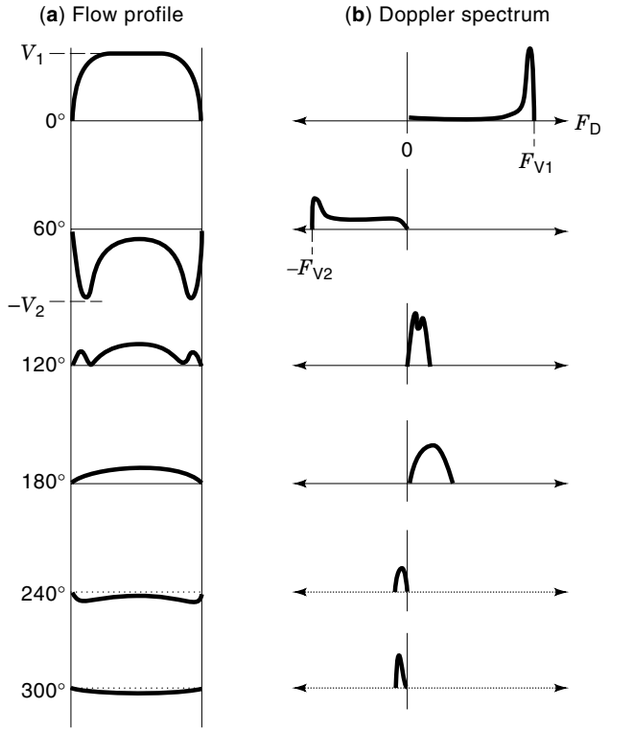

Figure 1. (a) Spatial flow profiles in the femoral artery. (b) Doppler spectra corresponding to the flow profiles in (a).

deeper tissues than from superficial ones, causing the average frequency in the Doppler spectrum to be shifted downward. The scattering of ultrasound by blood is proportional to the fourth power of frequency, which means that higher frequencies will be reflected at a higher amplitude than lower frequencies. Most systems are designed with the frequency dependence of tissue in mind, and the effect is usually considered insignificant (11).

The ultrasound signals travel through a number of different tissues and tissue interfaces before and after reflection from blood flow. There will be multiple reflections within these tissues, which can cause the echoes reflected from stationary tissues to arrive at the transducer at the same time as signals from moving blood. Additionally, there will be low-frequency components present from slow tissue motion, due to factors such as respiration, patient motion, and vessel wall motion. These low-frequency components are referred to as "clutter" and show up as very large amplitude, low-frequency components in the Doppler spectrum.

System Effects. The Doppler spectrum is also affected by the flow measurement system. Ideally, the sensitivity of the ultrasound beam generated and received by the transducer should be uniform across the ultrasound beam, which is not always the case. The beam pattern of an ultrasound transducer is quite complex near the front face of the transducer and becomes much more uniform in the far field. Differences in the sensitivity across the ultrasound beam will cause a biased representation of velocities within the ultrasound beam in the Doppler spectrum. Similarly, the ultrasound beam should be placed such that it passes uniformly through the diameter of the vessel of interest. If it does not, the blood flow in some parts of the vessel will be underrepresented, causing the Doppler spectrum to be distorted.

The Doppler shift is proportional to the transmitted frequency as well as the scatterer velocity. Depending on the system, the transmitted signal may be a single-frequency continuous tone as in a continuous wave system or short transmitted bursts of ultrasound as in a pulsed wave system. In the pulsed wave case, the transmitted burst will contain a band of frequencies, with an associated center frequency and bandwidth. All the frequencies in the transmitted frequency band will experience a Doppler shift, referred to as intrinsic spectral broadening. The amount of spectral broadening is affected by factors such as the transducer aperture size, finite observation time, and the angle between the ultrasound beam and flow. The degree of spectral broadening is important from a clinical standpoint because most Doppler measurements are made from the envelope of the Doppler spectrum.

Sonogram Doppler Spectral Display. The goal of a Doppler velocity measurement system is to take the information present in the Doppler spectrum and present it in a form useful to the clinician. Because the Doppler spectrum is in the audio range, the simplest output device is a speaker, where the clinician can listen to the "whooshing" sound of the Doppler signal and make assessments about the blood flow. A visual means of displaying the Doppler spectrum is to generate a spectral display, also commonly called a sonogram. A sonogram is a time-frequency plot where the horizontal axis represents time t, the vertical axis represents frequency f (sometimes calibrated as velocity), and the pixel brightness at position (t, f) represents the power in the Doppler spectrum at frequency f (and hence number of scatterers traveling at the velocity corresponding to f). A single vertical line at time t in a sonogram corresponds to the Doppler spectrum at time t. Figure 2(a) shows six vertical lines in a sonogram corresponding to the Doppler spectra for flow in the femoral artery shown in Fig. 1(b). The sonogram is a real-time display, where the clinician observes the sonogram trace as the transducer is placed upon a patient. Figure 2(b) shows the sonogram recorded from a pulsed wave Doppler system for flow in the carotid artery of a healthy human patient. The vertical axis is calibrated in frequency, and the Doppler frequency range is from -3.13 to $+3.13$ kHz. The vertical dotted lines indicate 1 s increments.

Mean Doppler Spectrum Frequency. The sonogram presents a large quantity of information, which is useful for qualitatively assessing blood flow. A more quantitative and important measurement is the mean frequency in the Doppler spectrum. The mean velocity in a blood vessel can be calculated from the mean frequency using Eq. 2 if the measurement angle is known, and when multiplied by the cross-sectional area of the vessel, the volumetric flow within the vessel can be calculated. The most common method of extracting the mean frequency from the Doppler signal is the intensity weighted mean frequency:

$$\overline{\omega}(t) = \frac{\int_{\omega} P(\omega)\omega\, d\omega}{\int_{\omega} P(\omega)\, d\omega} \tag{4}$$

where $P(\omega)$ is the Doppler power spectrum and $\omega = 2\pi f$.

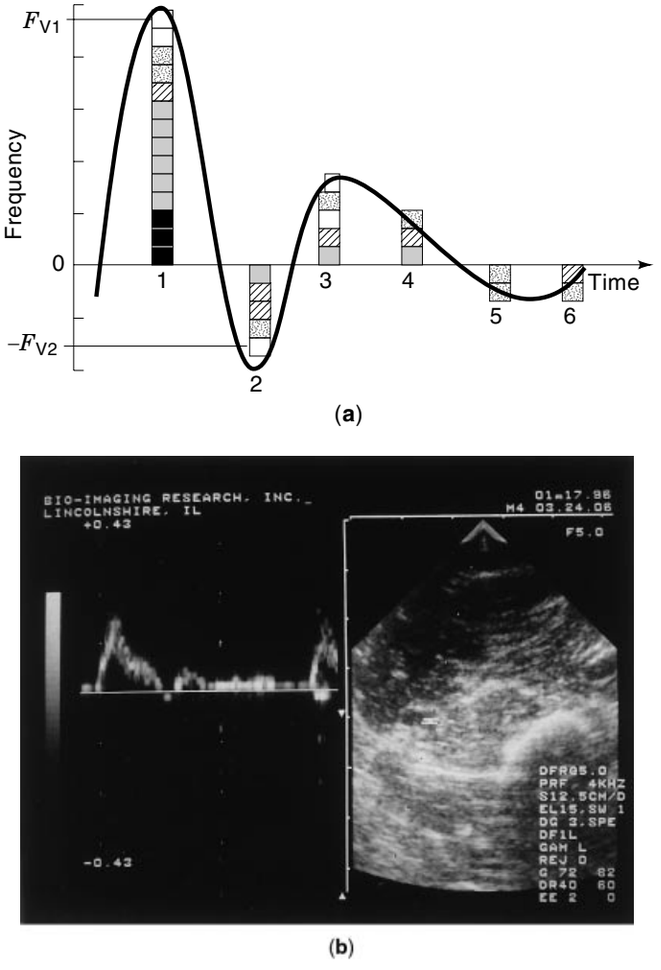

Figure 2. (a) Sonogram corresponding to the Doppler spectra for femoral flow in Fig. 1. (b) Actual sonogram obtained from a human carotid artery.

Doppler Velocity Measurement Systems

There are three classes of Doppler flow measurement systems: continuous wave (CW), pulsed wave (PW), and color flow mapping (CFM). All of them, except for the simplest CW systems, are typically capable of generating a sonogram as well as producing an audio output.

The CW Doppler system is the simplest and least expensive. A CW system consists of a transducer with separate transmit and receive elements, where the transmit element sends a single frequency of ultrasound continuously into the body and the receive element receives echo signals reflected from the body. The simplest CW system is a stand-alone unit consisting of a two-element probe and audio outputs to a speaker, tape recorder, or chart recorder. This type of unit has no means (other than visual placement of the probe) to determine where the beam is directed. CW Doppler systems can also be found on many ultrasound imaging systems, which helps in determining the location of the measurement in tissue.

A major limitation of CW Doppler is that it produces an average Doppler spectrum output for *all* flows within the beam and cannot provide any range information about the flow. If there are two vessels within the ultrasound beam, the resulting Doppler signal will represent the average flow over both vessels but cannot provide any information about the flow in the individual vessels. A PW Doppler system overcomes this limitation by pulsing a single transducer and using that same transducer to listen for echoes from flowing blood. Using a technique called range gating, it can provide flow information at specific ranges along the ultrasound beam. A PW Doppler system is incorporated into an ultrasound imaging system, where, in addition to Doppler processing, the ultrasound beam is scanned through tissue in order to create a gray-scale image of tissue structure. The combination of structure imaging and the sonogram is commonly referred to as duplex imaging, where the display is split into two parts: the gray-scale tissue image and the sonogram, as shown in Fig. 3. The tissue image is on the right-hand side of the video display, with the sonogram on the left. Controls on the imager allow placement of a cursor anywhere in the tissue image. In Fig. 3, the scanning transducer has been oriented such that the cross section of the brachial artery appears in the tissue image, and an I-shaped cursor has been placed inside the lumen of the vessel. The length of the cursor determines the sample volume size and can be adjusted by the user. A small sample volume size (as shown) can be used to measure the peak flow at the center of the vessel. Conversely, the sample volume can be increased to encompass the whole vessel, thereby measuring the average flow. On many machines, the physician can listen to the output while watching the sonogram. The display can typically be adjusted such that only the image, only the sonogram, or both are displayed. Most machines also have a video output and video recorder, so that the image and sonogram can be recorded and later reviewed.

A CFM system is based on PW Doppler techniques and usually includes all the features of a PW system but takes the range-gating technique one step further. It measures the Doppler frequency at many locations in the ultrasound image rather than at one individual cursor location. It converts the Doppler frequency at each point into a color; typically (but not

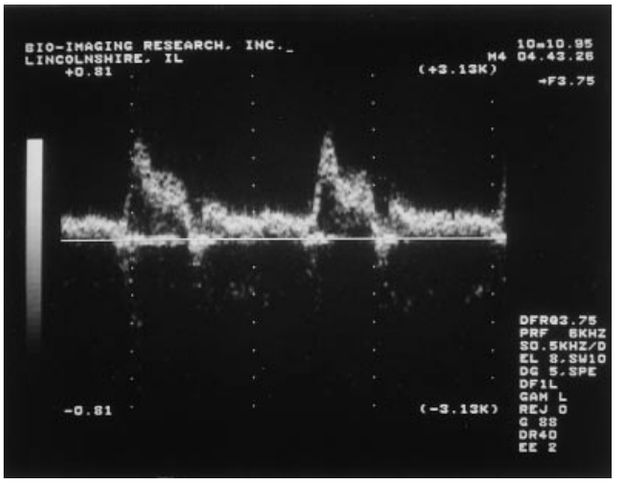

Figure 3. Sonogram (left) of flow in a human brachial artery and real-time ultrasound image (right) of the cross section of the artery in the arm. The sonogram vertical Doppler frequency scale is in kilohertz, and the vertical dotted lines represent 1 s time intervals.

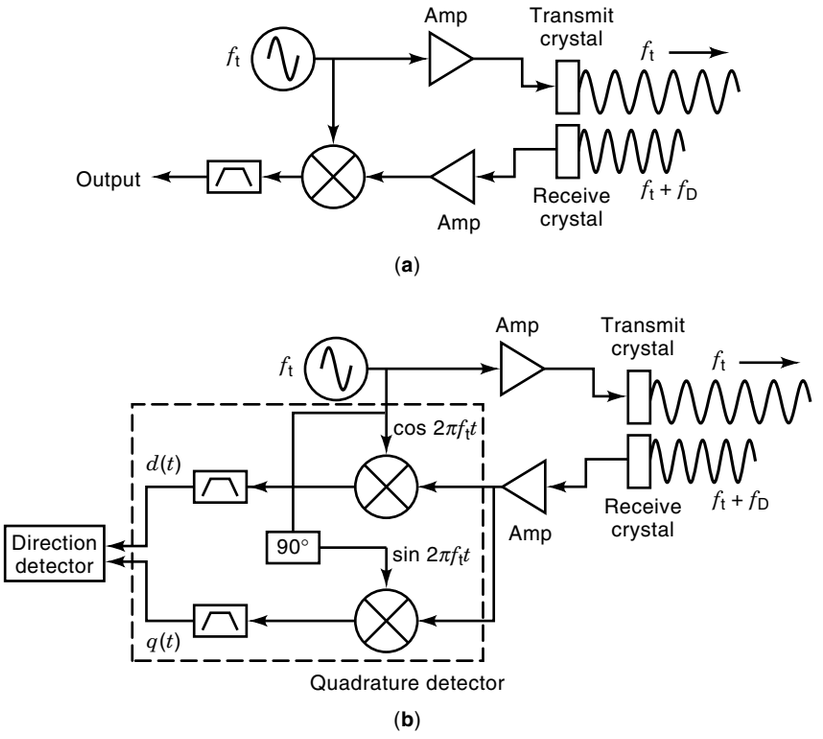

Figure 4. Block diagram of (a) nondirectional CW Doppler system based on Satomura (2) and Franklin et al. (4). (b) CW Doppler with quadrature detection developed by McLeod (5).

always) it uses blue for positive flow toward the transducer and red for negative flow away from the transducer. The brightness of the color is proportional to the magnitude of the Doppler frequency. Color flow imaging thus produces a real-time image of flow over a large spatial area rather than a sonogram at a single physical point.

Continuous Wave Doppler. The first nondirectional continuous wave systems were developed by Satomura in 1957 (2) and Franklin et al. in 1961 (4). The block diagram of a nondirectional Doppler system in shown Fig. 4(a). Two separate transducer elements are required: one for transmit and one for receive. A master oscillator with frequency f_t is used to electricaly excite the transmit element continuously. The element produces a longitudinal acoustic wave, which propagates in tissue and is reflected back toward the transducer by both stationary and moving reflectors within the body. The reflected echoes are converted back into electrical energy by the receive element, and mixing the received signal with the transmitted signal produces both the sum and difference of the transmitted and received signals. The bandpass filter removes the DC component from stationary tissue and the high-frequency sum component, leaving only the Doppler difference signal. A serious limitation of this system is that directional information is lost in the demodulation process. The first direction Doppler system, developed by McCleod in 1967 (5), is shown in Fig. 4(b). The received signal is split into two channels: a direct channel and a quadrature channel. The direct channel mixes the received signal directly with the oscillator signal (cos $2\pi f_t$), and the quadrature channel mixes it with the oscillator channel phase shifted by 90° (sin $2\pi f_t$). After demodulation and filtering, the direct channel $d(t)$ will lag the quadrature channel $q(t)$ by 90° if the flow is in the direction of the probe and lead the quadrature channel by 90° if the flow is away from the probe. The quadrature phase detected signals are further processed by direction detection circuitry to fully separate the forward and reverse flow components. Three primary methods of direction detection are employed: time-domain processing, phase-domain processing, and frequency-domain processing. Time-domain processing was implemented by McLeod and employs a logic circuit to determine whether the $d(t)$ or $q(t)$ signal is leading or lagging. The output of the logic circuit flips an electronic switch, which sends the Doppler flow signal to either the forward or reverse flow channel. The time-domain processor will not work correctly when both forward and reverse flow signals are present because the relationship between $d(t)$ and $q(t)$ is indeterminate. To overcome this problem, Nippa et al. (6) and Coghlan and Taylor (7) developed phase-domain processing means, shown in Fig. 5(a), to extract the forward and reverse flow components. The phase-domain processing phase shifts both the direct and quadrature channels by 90° and adds them to the other channel, producing separate forward and reverse flow channels. Both time- and phase-domain processing produce dual outputs; a single output can be produced using frequency-domain processing (7), as shown in Fig. 5(b). Here the direct and quadrature signals are mixed with quadrature signals from a pilot oscillator, which produces the forward and reverse flow components separated on either side of f_p.

Early CW systems used analog means to estimate the mean frequency, and one of the most popular methods was the zero-crossing detector developed by Franklin et al. (4). The zero-crossing detector counts the number of times the Doppler audio signal crosses its mean value and, under ideal conditions, produces an analog output proportional to the root-mean-square frequency of Doppler signal. The zero-crossing detector, however, is very susceptible to noise, and its performance is poor when the Doppler spectrum contains a wide

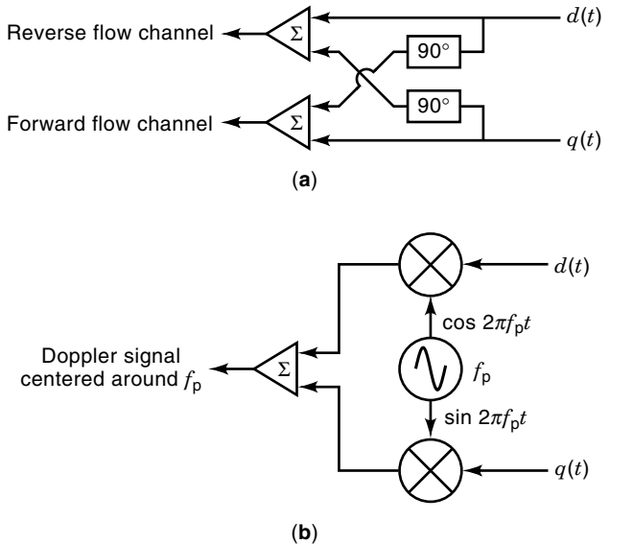

Figure 5. Direction determination in Doppler systems. (a) Phase-domain processing [Nippa et al. (6) and Coghlan and Taylor (7)]. (b) Time-domain processing [Coghlan and Taylor (7)].

range of frequencies. Currently, most systems determine the Doppler spectrum with real-time spectral analysis. Early systems incorporated analog means such as swept filter analyzers and parallel filter analyzers; most modern systems digitize the Doppler signal and calculate the FFT in order to obtain the Doppler spectrum.

Pulsed Doppler Systems. The first range-gated pulse Doppler systems were introduced by Wells (8) and Peronneau and Leger (9) in 1969 and in 1970 by Baker (10). A pulsed Doppler system incorporates a single transducer to transmit ultrasound pulses sequentially and listen to echoes, as shown in Fig. 6. A narrow-band signal, typically a 3 to 10 cycle pulse train with frequency f_t, is transmitted at a pulse repetition frequency (PRF). The distance, or range, to the blood cells is determined by range gating. When the ultrasound pulse is transmitted, the transmission time is noted, and the round trip time t_{rt} for any section of received echo can be calculated. The distance to a section of echo is

$$d = \frac{ct_{rt}}{2} \tag{5}$$

where c is the speed of sound in tissue.

Doppler Signal Sampling. In practice, pulsed Doppler systems sample the Doppler signal at the PRF rate by comparing the phase of the received echo with the reference transmitted signal. A block diagram of a unidirectional pulsed Doppler system is illustrated in Fig. 7. The transmitted signal is created by gating and amplifying the output of the reference signal at the desired PRF rate. The received signal is amplified and demodulated by multiplication with the center frequency of the transmitted pulse. The demodulated signal is bandpass filtered and sampled at a delay of t_{rt} after the transmitted pulse, which corresponds to the received echo at the desired range. Sampling of the Doppler signal is shown in Fig. 8 for a range-gated distance d. As scatterers move past the sampling position, the phase of the reflected echo will change with respect to the transmitted pulse. This phase is sampled from the demodulated signal once for every pulse transmission at the dotted lines. If there is no motion at the range-gated location, the demodulated signal will remain constant, and the output will remain at a constant value. There is some argument as to whether this phase measurement measures the "true" Doppler effect (11); however, the resulting sampled signal is representative of the Doppler signal and used in the Doppler velocity equations.

Wall Filter. In addition to removing the unwanted frequency components caused by mixing, additional filtering is required to remove clutter components. This filter is typically referred to as a wall filter because much of the undesired low-frequency clutter components are caused by reflections from the vessel walls. The design of the high-pass wall filter must be made such that the spectral content of the desired Doppler signal is distorted as little as possible. The complexity of the wall filter design is determined by such factors as the pro-

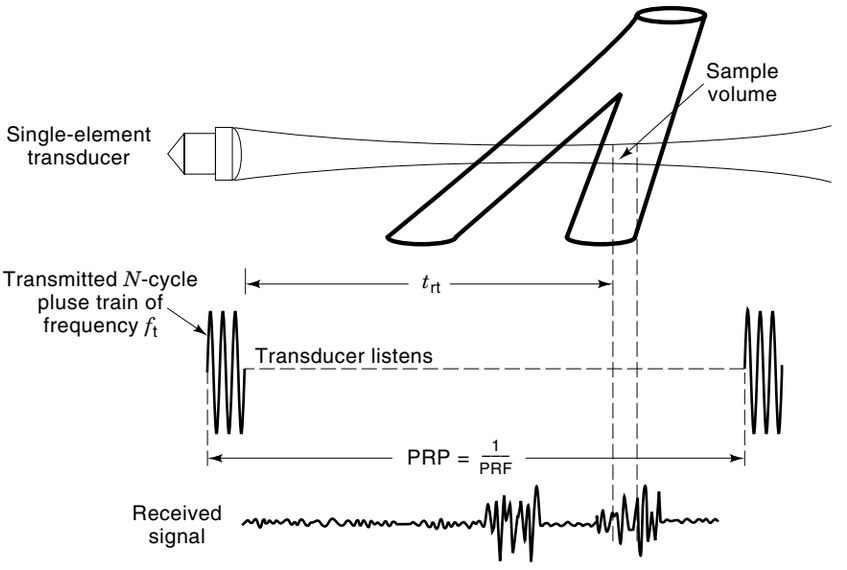

Figure 6. Pulsing, receiving, and range-gating of ultrasound signals in a pulsed wave Doppler system.

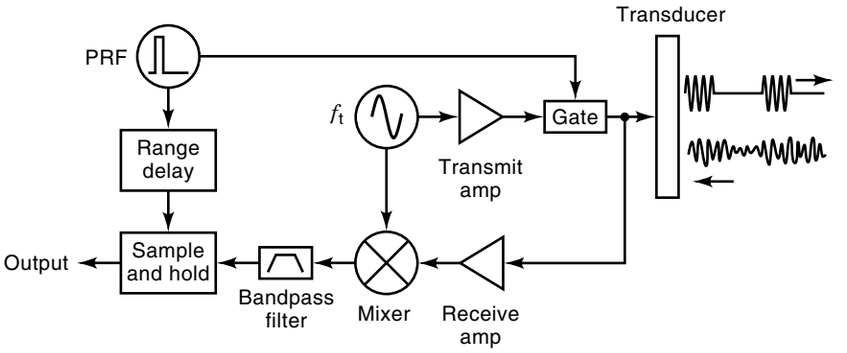

Figure 7. Unidirectional pulsed wave Doppler flow measurement system, based on Baker (10).

cessing time available and the blood flow velocities present. On many systems, the user can adjust the frequency cut-off of the wall filter.

Spectral Resolution. The resolution of the PW Doppler spectrum depends on the number of Doppler signal samples, which is determined by the pulse packet. In Fig. 8, a pulse packet of M samples is shown. This packet consists of M transmitted pulses and M consecutive samples of the Doppler signal. Obviously, the Doppler spectrum cannot be calculated from a single pulse ($M = 1$), and a larger pulse packet will produce a higher-resolution Doppler spectrum. Because the Doppler signal is sampled at a rate given by the PRF, the spectral resolution with an M pulse packet is given by

$$\Delta f = \frac{1}{M \cdot \text{PRP}} \tag{6}$$

where PRP = 1/PRF. We assume that the flow is stationary over the acquired data interval. For arterial flow, the Doppler signal can be considered stationary for periods less than approximately 10 ms; thus the data acquisition time $M \times$ PRP must be less 10 ms. Typical pulse packet sizes are 50 to 100 pulses.

Additionally, Doppler information must be acquired and displayed in real time along with the ultrasound image. The imager typically obtains 128–256 lines of image data and creates a real-time image from the data at frame rates on the order of 20 to 30 frames/s. There must be enough time for the system to both create and display the image along with the Doppler spectrum data. For PW systems, this is not a difficult time constraint because the Doppler spectrum is measured at only one point.

Averaging. The ultrasound echoes reflected from blood are very low in magnitude, typically 40 dB below that of surrounding tissue, which means that the signal-to-noise ratio of Doppler signals is also very low. Increasing the number of points in the pulse packet increases the spectral resolution, but has only a small effect on the signal-to-noise ratio (SNR). In order to improve the SNR, different independent measurements of the Doppler spectrum must be averaged. Pulsed Doppler machines use a number of different averaging strategies to improve the SNR (3). One of these is to break up the M-length data segment into smaller N-length data segments and average the Doppler spectra calculated from the N-length segments. The resolution of the averaged Doppler spectrum is smaller, but the SNR is improved. Another method is to keep the data length at maximum and synchronize the averaging with the heartbeat. M-length data segments can be acquired only at peak systole, for example. Because the data are acquired over a short interval at the same point in the cardiac cycle, they can be averaged without violating the stationarity criterion.

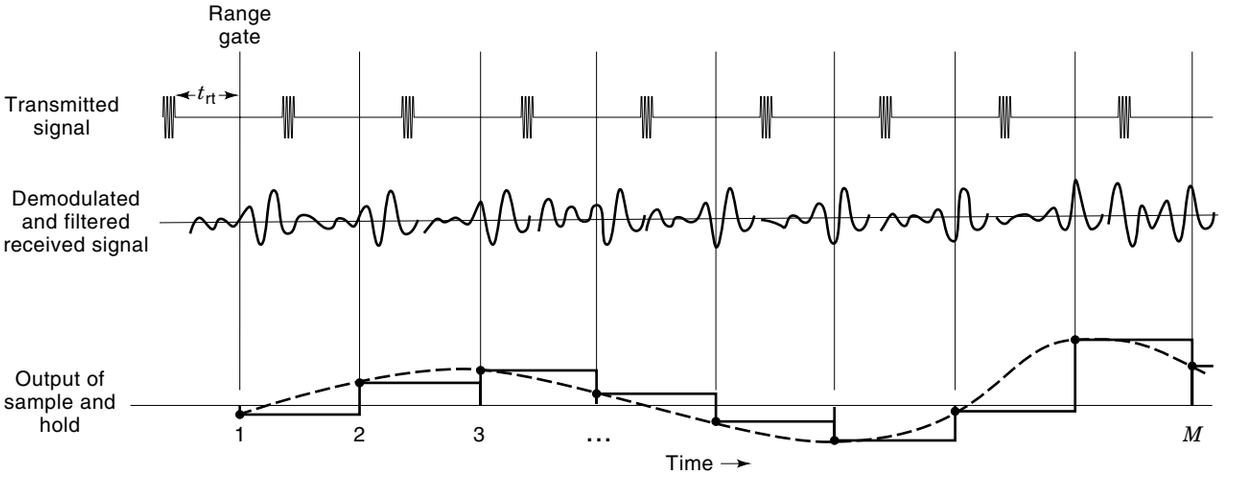

Figure 8. Sampled output of a pulsed wave Doppler system. The output for an M-length pulse packet is shown.

Pulsed Doppler Limitations. Pulse Doppler systems have a number of limitations not found with CW Doppler systems. When the transducer is in listen mode and receives an echo, it does not know whether the echo is a result of the preceding transmitted pulse or earlier transmitted pulses. It must be guaranteed that all echo signals resulting from a given transmitted burst are received in time *before* the next burst is transmitted, or else there will be *range ambiguity.* For a given PRF, the maximum depth for unambiguous flow measurement is

$$D_{\max} = \frac{c}{2\,\mathrm{PRF}} \tag{7}$$

Additionally, the phase of the returning ultrasound echoes is determined by comparing the phase between the reference oscillator and the returning ultrasound echo signal. This limits the maximum observable phase change to $\pm 180°$. This limit is simply an expression of the Nyquist theorem, which states that, in order to sample a signal accurately, the frequency of sampling must be at least twice the maximum frequency in the signal to be sampled. Because the Doppler signal is sampled at the PRF rate, the highest Doppler shift that can be measured is

$$f_{\mathrm{D}}(\max) = \frac{\mathrm{PRF}}{2} \tag{8}$$

Combining this with Eq. (2) determines the *maximum velocity* that can be measured for a given PRF:

$$V_{\max} = \frac{c\,\mathrm{PRF}}{4 f_{\mathrm{t}} \cos\theta} \tag{9}$$

If the blood flow velocity exceeds $V_{\max}$, aliasing will occur. Aliasing occurs when the frequency of a sampled signal exceeds the Nyquist rate, causing the sampled signal to appear incorrectly as a lower-frequency signal. In a PW Doppler system with quadrature detection, the Doppler frequency can be positive or negative, and unaliased Doppler frequencies exist between $-$PRF/2 and $+$PRF/2. The effect of aliasing in this case is that when f_{D} exceeds $+$PRF/2, it is incorrectly mapped to $-$PRF/2, and frequencies above $+$PRF/2 are mapped into the $-$PRF/2 to PRF/2 range. Some PW Doppler machines have the ability to shift the sonograms graphically. Instead of displaying the sonogram from $-$PRF/2 to $+$PRF/2, for example, the sonogram range can be shifted to display from 0 to $+$PRF, or from $-$PRF/4 to $+3$ PRF/4, as long as the total range remains PRF. The permissible range of frequencies is not changed; only the way the frequencies are mapped onto the frequency scale is changed.

Equation (7) indicates that a low PRF is desirable in order to measure flow at deep locations in the body; and Eq. (9) indicates that a high PRF is desirable in order to measure high velocities. Thus a tradeoff must be made between the maximum depth of measurement and maximum velocity measurement. Equations (7) and (9) can be combined to give the *maximum range-velocity limit:*

$$D_{\max} V_{\max} = \frac{c^2}{8 f_{\mathrm{t}} \cos\theta} \tag{10}$$

This limit states that for a given operating frequency f_{t} and desired depth in tissue $D_{\max}$, velocities above $V_{\max}$ cannot be unambiguously measured.

Color Flow Mapping Systems. A CFM system uses PW Doppler techniques to generate a color-coded map of flow velocities. This color-coded map is combined with the gray-scale ultrasound image of the anatomy. Unlike a sonogram at a single range gate produced by a PW system, a color flow image consists of thousands of range gate locations where the mean frequency of the Doppler spectrum is measured. This vast number of measurement locations places a tremendous processing challenge on CFM systems. In order to meet this challenge, the techniques used in conventional PW Doppler systems have been significantly modified and optimized for speed.

A major difference between a CFM system and a PW Doppler system is that, for the CFM case, the ultrasound beam remains at a given location for only a very short time. In a PW Doppler system, the range gate location is essentially stationary until the operator moves the sample volume cursor. In a CFM system, the beam is continually swept in order to produce the spatial color flow map. For example, if an ultrasound image consists of 128 lines in the sweep with a frame rate of 20 frames/s, a range gate position can be held along any given line for only 0.4 ms. Because the resolution of the Fourier spectrum is the reciprocal of the data segment length, the resolution of the Doppler spectrum will be very crude at only 2.5 kHz.

Autocorrelation Technique. In order to circumvent this problem, an autocorrelation technique, first described by Namekawa et al. (12) in 1982 and further developed by Kasai et al. (13) in 1985, is used in most CFM systems (3). The autocorrelation magnitudes and phases at $\tau = 0$ and $\tau = T$ are used to calculate the mean frequency and variance of the Doppler signal. The mean frequency of the Doppler power spectrum is given in Eq. (3), and the variance of the estimate is given by

$$\sigma^2(t) = \overline{\omega^2} - (\overline{\omega})^2 = \frac{\displaystyle\int_\omega P(\omega)(\omega - \overline{\omega})^2\, d\omega}{\displaystyle\int_\omega P(\omega)\, d\omega} \tag{11}$$

The Doppler power spectrum $P(\omega)$ is related to the autocorrelation function $R(\tau)$ of the Doppler signal by the Wiener-Kinchin theorem:

$$R(\tau) = \int_\tau f_{\mathrm{D}}(t) f_{\mathrm{D}}(t-\tau)\, dt \tag{12}$$

$$= \int_\omega P(\omega) e^{j\omega t}\, d\omega \tag{13}$$

By calculating the autocorrelation of the time-domain Doppler signal, the mean frequency and variance can be written in terms of the autocorrelation function:

$$\overline{\omega} = -j\frac{R'(0)}{R(0)} \tag{14}$$

$$\sigma^2 = \left(\frac{R'(0)}{R(0)}\right)^2 - \frac{R''(0)}{R(0)} \tag{15}$$

where $R'(0)$ and $R''(0)$ are the derivatives of $R(\tau)$ at zero lag. Further simplification is made by assuming that the phase of

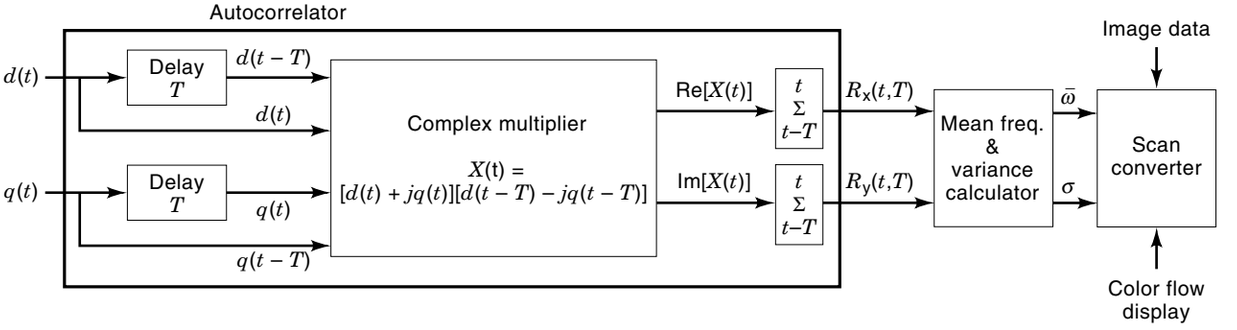

Figure 9. Block diagram of an ultrasound color flow mapping system, based on Kasai et al. (13).

$R(\tau)$ is linear with respect to time, and the mean frequency and variance are approximated as

$$\overline{\omega} = \frac{\phi(T)}{T} \tag{16}$$

$$\sigma^2 = \frac{2}{T^2}\left(1 - \frac{|R(T)|}{R(0)}\right) \tag{17}$$

where T is in units of the PRP and $\phi(T)$ is the phase of the first lag of the autocorrelation.

The block diagram of a basic CFM system is shown in Fig. 9. The receiving and demodulation electronics of a CFM system are similar to that of a standard PW system, and the inputs to the autocorrelator are the digitized quadrature detected signals $d(t)$ and $q(t)$. The outputs of the autocorrelator are the real and imaginary parts $R_x(t, T)$ and $R_y(t, T)$ of autocorrelation function. The phase and magnitude are calculated by

$$\phi(t, T) = \tan^{-1}\frac{R_y(t, T)}{R_x(t, T)} \tag{18}$$

$$|R(t, T)| = \sqrt{R_x^2(t, T) + R_y^2(t, T)} \tag{19}$$

$$R(t, 0) = \sum_{t-T}^{t} d^2(t) + q^2(t) \tag{20}$$

The mean frequency and variance information is fed into a scan converter, which converts the phase to a color. Typically (but not always), negative phases are encoded as blue and positive phases as red (corresponding to flow toward or away from the transducer), with the brightness of the color related to the magnitude of the phase (corresponding to the flow velocity magnitude). The color flow map is combined with the gray-scale image map in the scan converter to produce the total color flow image display.

Color Flow Limitations. Because color flow imaging systems are based on PW principles, they also have the same limitations. The Doppler shift is still determined by Eq. 2, which means that the angle θ must be known. For PW systems, this is usually estimated from the position of the Doppler scan line in the image. With color flow systems, the flow is measured along many scan lines, and the angle changes between scan lines, particularly for a sector scan image. This can cause image artifacts, which the operator must be aware of. If a vessel is longitudinally oriented in a sector scan image, typically one of the sector scan beams will be at a 90° angle with the vessel. Thus, the flow will be toward the transducer for beams on one side of the 90° beam, away for those on the other side, and zero at 90°. The corresponding color flow image will indicate that the flow stops and reverses direction in the vessel (red on one side of 90°, black at 90°, and blue on the other side). Some machines incorporate angle correction into the system. The user aligns a cursor with the vessel axis to estimate θ, which is then used in the velocity estimation equations. Color flow images are also limited by aliasing, as well as the maximum range-velocity limits of PW systems. As with PW systems, aliasing causes velocities that are too high for the PRF to be flipped over to the reverse channel. In color flow systems, this will cause a high velocity, which should be mapped as red to be mapped into blue.

In order to produce the real-time display, CFM systems incorporate other tradeoffs with respect to PW systems. In a PW system, the packet size is 50 to 100 or more pulse trains. However, because of time constraints, the pulse packet size for a CFM system is on the order of 8 pulse trains. The clinical implications of a small packet size is that velocity resolution is sacrificed because the spectral resolution is directly related to the number of pulses making the spectral estimate. The temporal resolution is also lower for a CFM system because it is determined by how often the mean velocity is sampled at any given point.

Power Mode Images. Many CFM imagers can also display a *power* image as well as a color flow image (14). A power image maps the power [$R(0)$ in Eq. (20)] of the Doppler shift rather than the Doppler shift itself. A power image contains no velocity or direction information, and basically it indicates only where there is motion present. It has the advantage that the power is not dependent on the transducer-flow angle θ and is not affected by aliasing, and thus has a better SNR than regular color flow images. This allows smaller and more complex vessels to be imaged.

TIME-DOMAIN VELOCITY MEASUREMENT

The first ultrasonic blood flow measurement systems, as well as most current commercial systems, are based on Doppler principles. A more recent development, incorporated in a few machines, is based on time-domain correlation. Correlation methods estimate the time shift, rather than the frequency shift, of echoes reflected from moving scatterers. Cross correlation is a common method used to measure the arrival time

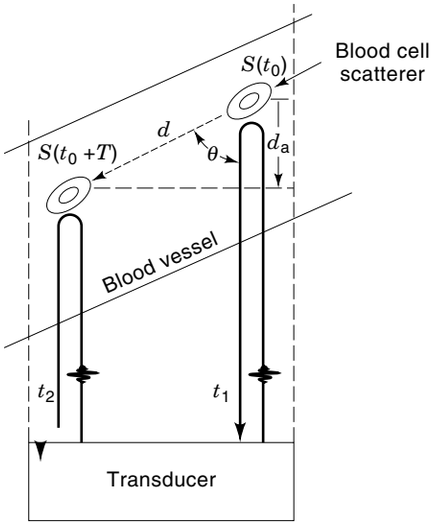

Figure 10. Ultrasound time-domain velocity measurement concept. The velocity is estimated from the round-trip time it takes an ultrasound pulse to travel to the scatterer and back to the transducer for multiple scatterer positions.

and delay of electronic signals and has been extensively used in radar and sonar applications since the 1950s. Dotti et al. (15) reported the first use of ultrasonic cross correlation for medical flow measurement in 1976, and later systems were described by Bonnefous and Pesque (16), Foster et al. (17), and Embree and O'Brien (18).

Time-Domain Flowmeter Concept

Figure 10 illustrates the ultrasound time-domain flowmeter concept. Here an ultrasound transducer is oriented at an angle θ with respect to a blood vessel. At time $t = t_0$, a blood cell scatterer S is located at position $S(t_0)$. When an ultrasonic pulse is transmitted, it takes a round trip time t_1 to leave the transducer, get reflected, and return to the transducer. When another ultrasonic pulse is transmitted at time $t = t_0 + T$, the scatterer will have moved to position $S(t_0 + T)$ and the round trip transit time will be t_2. The axial distance d_a the scatterer has moved is

$$d_a = \frac{(t_1 - t_2)c}{2} \tag{21}$$

where c is the speed of sound in the medium. The true distance d the scatterer has moved down the vessl is

$$d = d_a \cos\theta \tag{22}$$

and the true scatterer velocity is (assuming $V_T \cos\theta \ll c$)

$$V_T = \frac{(t_1 - t_2)c}{2T\cos\theta} \tag{23}$$

This time-domain equation is identical to the Doppler Equation (1), except that it has a change in time in the numerator instead of a change in frequency and a pulse repetition period in the denominator instead of the transmitted frequency. The change in time $t_1 - t_2$ is referred to as the time shift and is denoted by the variable τ. Note that as with Doppler systems, it is the axial component of flow that is measured and time-domain correlation flowmeters of this type also cannot measure the flow at angles of 90°.

In real life, the spatial resolution of ultrasound in the 1 to 10 MHz range is much too small to resolve a single blood cell, and echoes are due to the combined effects of thousands of blood cells reflecting the ultrasound. The time-domain flowmeter concept for this case is illustrated in Fig. 11. Here, a *volume* of scatterers V moves down the blood vessel. At time t_0, the volume is totally within the ultrasound beam at position $V(t_0)$; and E_1 is the echo acquired at $t = t_0$. At $t = t_0 + T$, the volume has moved to the position $V(t_0 + T)$, with corresponding echo E_2. If the pulse repetition period T is set such that some of the original scatterers remain in the beam for both pulses [shaded areas of $V(t_0)$ and $V(t_0 + T)$], then these volume sections will produce similar sections of echo in E_1 and E_2 (shown in bold). These similar sections of echo will be displaced in time from each other by the time shift τ. Because blood reflects ultrasound as a Gaussian random variable (19), any small volume of blood cell scatterers will have its own unique ultrasonic footprint, and the common sections of echo will represent reflections from the same volume of blood cell scatterers.

Correlation Search

The time shift τ is estimated by a cross-correlational search through different echo signals. If $E_1(t)$ and $E_2(t)$ represent signals received at different times from a moving scatterer, then the correlation search can be pictured as shifting E_1 in time by some value of s and multiplying by E_2 to produce the correlation coefficient $R(s)$. The value of s is varied until a maximum in the value of $R(s)$ is found. Mathematically the correlation can be expressed as

$$R(s) = \int_t E_1(t+s)E_2(t)\,dt \tag{24}$$

The value of s that produces a maximum in the correlation function $R(s)$ corresponds to the time shift $s = \tau = t_1 - t_2$, and Eq. (3) is used to calculate the scatterer velocity.

Digital Correlation. The time shift τ is estimated at different ranges by a digital correlation search that finds the value of s producing the maximum $R(s) = R_{max}$. The correlation search process for digitized radiofrequency (RF) echo signals is shown in Fig. 12. A window $W_1(r)$ of length w samples is removed from source echo E_1 at a distance r points (corresponding to the desired range) from the beginning of the echo signal. The window length w and the transducer beam width define the sample volume size. A w-point correlation $W_1(r) \times W_2(r + s)$ is calculated, where $W_2(r + s)$ is a window in the search echo E_2. The correlation is calculated over the range of $-r \le s \le L - w$, and the value of s where the correlation function $R(s) = R_{max}$ corresponds to the time shift in discreet units of the A/D sampling period. The normalized w-point correlation coefficient $R(s)$ is given by

$$R(s) = \frac{\sum_{i=0}^{w-1} E_1[r+i]E_2[r+s+i]}{\sqrt{\sum_{j=0}^{w-1}(E_1[r+j])^2 \sum_{k=0}^{w-1}(E_2[r+s+k])^2}} \tag{25}$$

where E_1 and E_2 are the base addresses of the digitized echo signals. This equation estimates the similarity of the two win-

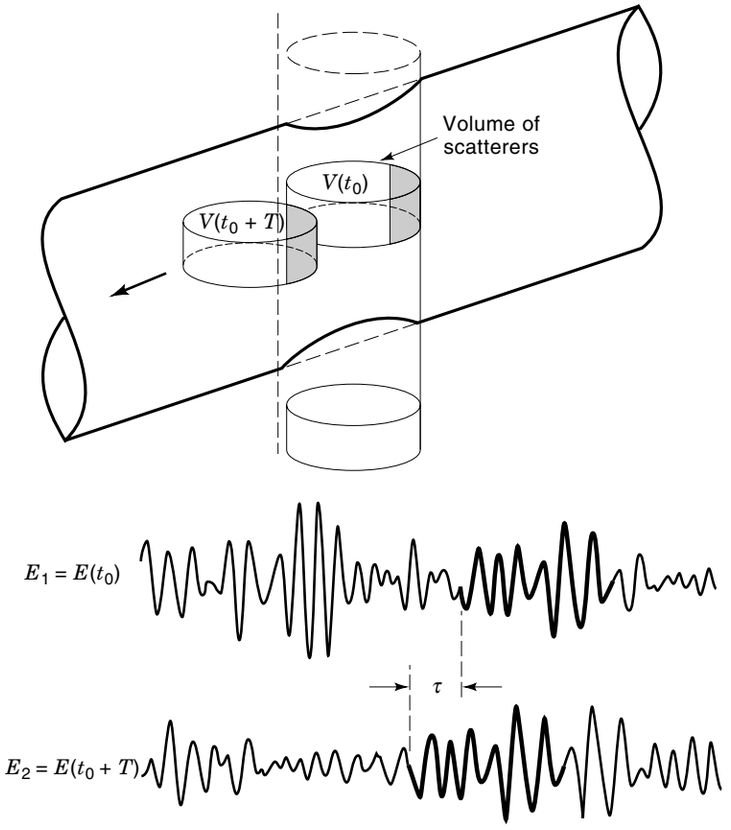

Figure 11. Ultrasound time-domain flow measurement with multiple scatterers. Volumes of scatterers present in the ultrasound beam for multiple pulses will have similar footprints in the received echoes, except shifted in time.

dows and produces a value between +1.0 and −1.0. A value of +1.0 corresponds to identical windows, zero indicates that the echoes are maximally dissimilar. The true location of R_{max} in general will not occur at the discreet locations where $R(s)$ is calculated but rather somewhere in between. In practice, a curve, such as a parabola, is fit to the maximum discreet point and its two neighbors, and the true maximum is estimated from the peak of the curve.

The correlation process can be performed on either the RF echo signal or envelope-detected signal. A system based on envelope-detected correlation is easier to implement because the envelope-detected signal is of lower frequency, and digitization requirements are not as stringent. The tradeoff is that the strong cyclic RF-component is lost, which produces a less accurate result.

Comparison of Time Domain and Doppler. The pulsing and range gating of ultrasound signals for time-domain correlation systems is similar to that for PW Doppler systems, except that the transmitted burst is a wideband signal, where the transducer is shock excited with as short an electrical signal as possible (as compared to the 3 to 10 cycle transmitted pulse for Doppler systems). This has spatial resolution implications because the spatial resolution is in part determined by the length of the transmitted pulse. The shorter ultrasound pulse transmitted by a time-domain system will theoretically have a better resolution than the longer pulse for Doppler systems.

One disadvantage of time-domain correlation is that it is computationally intensive. In practice, the normalization provided by the square-root term in the denominator is not needed to simply determine where the maximum occurs. Further increases in processing speed are obtained using a smaller number of bits in the correlation, as well as other comparison techniques such as the sum-absolute difference.

Theoretical research has shown that under poor SNR conditions, time-domain correlation performs better than Doppler. This may be important because signals from blood are typically very low in magnitude. Better performance under poor SNR conditions means that less averaging will have to take place, which means a potentially higher frame rate in a CFM imager.

Time-domain correlation techniques also do not suffer from aliasing. With time-domain correlation, the maximum measurable velocity is determined by how long the scatterers stay within the ultrasound beam. For similar systems, the maximum theoretical measurable velocity appears to be larger for time-domain systems.

The frequency-dependent attenuation and scattering of intervening tissue has the effect of biasing the Doppler spectrum. With time-domain correlation, each echo is affected in the same way, and the location of the maximum is thus unaffected by this frequency dependence.

Finally, the direction of the flow falls out naturally from the correlation process. A negative flow will have a negative time shift, and no additional hardware, such as quadrature detection, is required.

CONTRAST AGENTS

A method of increasing the very low signal strength of echoes reflected from blood is to inject a contrast agent into the

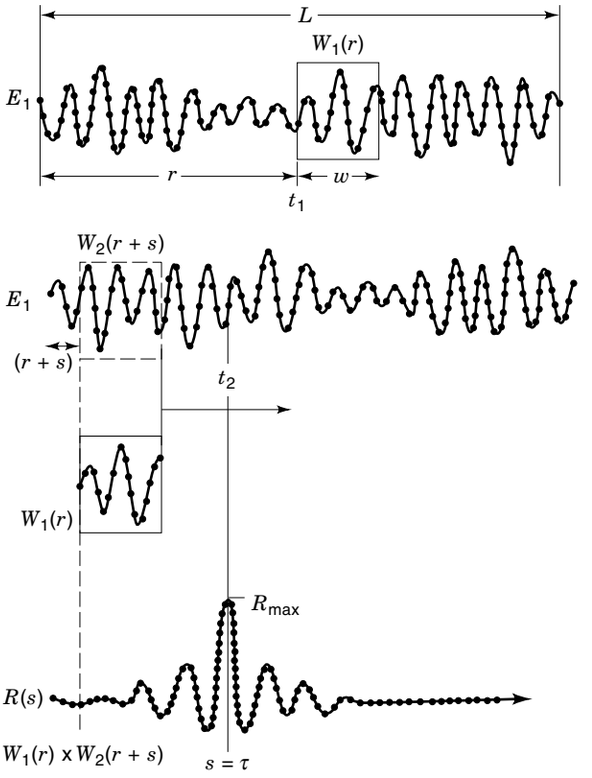

Figure 12. Correlation search process for a w-point range window $W_1(r)$ within E_1. The correlation $R(s) = W_1(r) \times W_2(r + s)$ is calculated at different search positions s within E_2. The search positions producing the maximum value for $R(s)$ corresponds to shifted position of W_1 in E_2.

bloodstream (20). A contrast agent consists of particles that have acoustically different characteristics (speed of sound, density, or absorption) than blood and thus enhances the backscattered signal from flowing blood. Most contrast agents consist of free or encapsulated nondifusable gas bubbles. The presence of the contrast agent causes an increase in brightness in an ultrasound image for organs where the blood containing the contrast agent is flowing. Currently, contrast agents are used extensively in ultrasonic echocardiographic applications. The presence of the contrast agent also increases the Doppler signal level, thereby improving Doppler color images and allowing potentially new applications such as perfusion measurement to be found. An important property of a contrast agent is its persistence, which determines how long it remains in the bloodstream before diffusing. Albunex, which is a currently FDA-approved contrast agent, remains detectable by ultrasound for a few minutes, whereas newer contrast agents can be imaged with ultrasound for hours.

EXPERIMENTAL AND FUTURE WORK

Doppler Spectrum Measurement

Currently, most Doppler machines estimate the Doppler spectrum by calculating the FFT from the Doppler signal. In addition to the "classical" FFT, "modern" spectral analysis techniques, such as the autoregressive (AR), moving average (MA), autoregressive moving average (ARMA), periodogram, and maximum likelihood (ML) models as well as the Wigner distribution function (WDF) also exist. These modern techniques show improved temporal resolution over the FFT under certain conditions at the cost of added complexity and increased computation time. Many of the modern techniques are characterized by a number of model parameters. The selection of the optimal number of parameters and parameter values is still under investigation and may change with the type of flow present. For these reasons, the FFT still remains the method of choice in determining the Doppler spectrum.

2-D and 3-D Techniques

Both the Doppler and time-domain correlation techniques, in their current commercial implementations, are capable of measuring only the *axial* component (the component in the direction of the ultrasound beam) of the true three-dimensional blood flow velocity vector and are thus unable to measure accurately blood flow at transducer-blood flow velocity vector angles near 90°. In order to overcome this limitation, a number of experimental techniques have been reported. They extend the basic Doppler and time-domain methods into two or three dimensions. Two- and three-dimensional techniques have the capability of measuring lateral components in addition to the axial component, allowing flow measurement at transducer-flow angles near 90°.

Multibeam Techniques. In order to measure lateral flow components, most techniques rely on multiple ultrasound beams. Multibeam Doppler techniques insonate the same physical location but from different directions. The Doppler technique is used to estimate the flow component along the two (or more) beams, thereby generating two or three velocity components rather than just one. Multibeam correlation techniques track volumes of blood cells as they move between ultrasound beams. Here the different ultrasound beams do not insonate the exact same volume, but nearby volumes. The lateral components of flow can be determined from the interbeam transit times.

Spectral Bandwidth. Newhouse et al. (21) have shown that the bandwidth of the Doppler spectrum bandwidth is also related to flow components in the transverse plane of an ultrasound beam. The Doppler frequency can thus be used to estimate the axial component of motion and the Doppler bandwidth the lateral component. This technique has the advantage that only one transducer is required to make 2-D measurements, and two for 3-D measurements.

High-Frequency Applications

The spatial resolution of ultrasound flow measurement systems is largely determined by the operating frequency, which, for commercial systems, is in the 1 to 10 MHz range. This frequency range limits the spatial resolution, which is on the order of 1.0 mm. Additionally, the minimum detectable flow is on the order of 10 mm/s. These limits preclude measurement of flow in small vessels where the flow rate is very low. Increasing the ultrasound frequency (at a cost of depth penetration) will increase the spatial resolution, as well as increase the Doppler shift frequency, making detection of low blood flow velocities easier. High-frequency ultrasound sys-

tems above 30 MHz cannot measure flows deep within the body, but they are ideally suited for measuring flows in small vessels near the front of the transducer. Potential applications include flow measurement in microcirculature near the skin, lymphatic system, and anterior structures of the eye.

BIBLIOGRAPHY

1. C. Doppler, Ueber das farbige Licht der Doppelsterne und einiger anderer Gestirne des Himmels. *Abhandl Konigl Bohm Ges Ser* **2**: 465–482, 1843.
2. S. Satomura, Ultrasonic Doppler method for the inspection of cardiac function. *J. Acoust. Soc. Amer.,* **29**: 1181–1185, 1957.
3. D. H. Evans, et al., *Doppler Ultrasound: Physics, Instrumentation, and Clinical Applications.* New York: Wiley, 1991.
4. D. L. Franklin, W. Schlegel, and R. F. Rushmer, Blood flow measured by Doppler frequency shift of back-scattered ultrasound. *Science,* **134**: 564–565, 1961.
5. F. D. McCleod, A directional Doppler flowmeter. *Dig. 7th Int. Conf. Med. Biol. Eng.,* 1967, p. 213.
6. J. H. Nippa, et al., Phase rotation for separating forward and reverse blood velocity signals. *IEEE Trans. Sonics Ultrason.,* **SU-22**: 340–346, 1975.
7. B. A. Coghlan and M. G. Taylor, Directional Doppler techniques for detection of blood velocities. *Ultrasound Med. Biol.,* **2**: 181–188, 1976.
8. P. N. T. Wells, A range gated ultrasonic Doppler system. *Med. Biol. Eng.,* **7**: 641–652, 1969.
9. P. A. Peronneau and F. Leger, Doppler ultrasonic pulsed blood flowmeter. *Proc. 8th Int. Conf. Med. Biol. Eng.,* 1969, pp. 10–11.
10. D. W. Baker, Pulsed ultrasonic Doppler blood-flow sensing. *IEEE Trans. Sonics Ultrason.,* **SU-17**: 170–185, 1970.
11. J. A. Jensen, *Estimation of blood velocities using ultrasound.* Cambridge: Cambridge University Press, 1996.
12. K. Namekawa, et al., Real-time bloodflow imaging system utilizing auto-correlation techniques, in R. A. Lerski and P. Morley (eds.), *Ultrasound '82.* New York: Pergamon, 1982.
13. C. Kasai, et al., Real-time two-dimensional blood flow imaging using an autocorrelation technique. *IEEE Trans. Sonics Ultrason.,* **SU-32**: 458–464, 1985.
14. H. F. Routh, Doppler ultrasound. *IEEE Eng. Med. Biol. Mag.,* **15** (6): 31–40, 1996.
15. D. Dotti, et al., Blood flow measurements by ultrasound correlation techniques. *Energia Nucleare,* **23** (11): 571–575, 1976.
16. O. Bonnefous and P. Pesque, Time domain formulation of pulse-Doppler ultrasound and blood velocity estimation by cross correlation. *Ultrason. Imaging,* **8**: 73–85, 1986.
17. S. G. Foster, P. M. Embree, and W. D. O'Brien, Jr., Flow velocity profile via time-domain correlation: Error analysis and computer simulation. *IEEE Trans. Ultrason. Ferroelectr. Freq. Control,* **37**: 164–175, 1990.
18. P. M. Embree and W. D. O'Brien, Jr., Volumetric blood flow via time-domain correlation: Experimental verification. *IEEE Trans. Ultrason. Ferroelectr. Freq. Control,* **37**: 176–189, 1990.
19. B. A. J. Angelson, A theoretical study of the scattering of ultrasound from blood. *IEEE Trans. Biomed. Eng.,* **BME-27**: 61–67, 1980.
20. N. de Jong, Improvements in ultrasound contrast agents, *IEEE Eng. Med. Biology Mag.,* **15** (6): 72–82, 1996.
21. V. L. Newhouse, et al., Ultrasound Doppler probing of flows transverse with respect to beam axis. *IEEE Trans. Biomed. Eng.,* **BME-34**: 779–789, 1987.

Reading List

Clinical Applications

K. J. W. Taylor, P. N. Burns, and P. N. T. Wells, *Clinical Applications of Doppler Ultrasound.* New York: Raven Press, 1995.

C. R. B. Merritt (ed), *Doppler Color Imaging.* New York: Churchill Livingstone, 1992.

K. J. W. Tayler (ed), *Duplex Doppler Ultrasound.* New York: Churchill Livingstone, 1990.

Time-Domain Methods

I. A. Hein, Current time-domain methods for assessing tissue motion by analysis from reflected ultrasound echoes—A review. *IEEE Trans. Ultrason. Ferroelectr. Freq. Control,* **40**: 84–102, 1993.

Ultrasound Scattering by Blood

L. Y. L. Mo and R. S. C. Cobbold, Theoretical models of ultrasonic scattering in blood, in K. K. Shung and G. A. Thieme (eds.), *Ultrasonic Scattering in Biological Tissues.* Boca Raton: CRC Press, 1993.

Doppler Spectrum Estimation

B. A. J. Angelson, Instantaneous frequency, mean frequency, and variance of mean frequency estimators for ultrasonic blood velocity Doppler signals. *IEEE Trans. Biomed. Eng.,* **28**: 733–741, 1981.

P. J. Vaitkus, R. S. C. Cobbold, and K. W. Johnston, A comparative study and assessment of Doppler ultrasound spectral estimation techniques part I: Estimation methods. *Ultrasound Med. Biol.,* **14** (8): 661–672, 1988.

L. Fan and D. H. Evans, Extracting instantaneous mean frequency information from Doppler signals using the Wigner distribution function. *Ultrasound Med. Biol.,* **20** (5): 429–443, 1994.

2- and 3-D Ultrasonic Blood Flow Measurement

G. E. Trahey, S. M. Hubbard, and O. T. von Ramm, Angle independent ultrasonic blood flow detection by frame-to-frame correlation of B-mode images. *Ultrasonics,* **26**: 271–276, 1988.

M. D. Fox and W. D. Gardiner, Three-dimensional Doppler velocimetry of flow jets. *IEEE Trans. Biomed. Eng.,* **35**: 834–841, 1988.

Z. Guo, et al., A quantitative investigation of in-vitro flow using three-dimensional colour Doppler ultrasound. *Ultrasound Med. Biol.,* **21**: 807–816, 1995.

V. L. Newhouse, et al., Three-dimensional vector flow estimation using two transducers and spectral width. *IEEE Trans. Ultrason. Ferroelectr. Freq. Control,* **41**: 90–95, 1994.

G. R. Bashford and O. T. von Ramm, Ultrasound three-dimensional velocity measurements by feature tracking. *IEEE Trans. Ultrason. Ferroelectr. Freq. Control,* **43**: 376–384, 1996.

I. A. Hein, 3-D flow velocity vector estimation with a triple-beam lens transducer—Experimental results. *IEEE Trans. Ultrason. Ferroelectr. Freq. Control,* **44**: 85–95, 1997.

High-Frequency Ultrasonic Flow Measurement

G. R. Lockwood, et al., Beyond 30 MHz: Applications of high-frequency ultrasound imaging. *IEEE Eng. Med. Biology Mag.,* **15** (6): 60–71, 1996.

K. W. Ferrara, et al., Estimation of blood velocity with High Frequency Ultrasound. *IEEE Trans. Ultrason. Ferroelectr. Freq. Control,* **43**: 149–157, 1996.

ILMAR A. HEIN
Bio-Imaging Research, Inc.